SciencePG
Science Publishing Group

An Energy Criterion for Rheological Failure of Rock and Application in Stability Analysis of Natural High Slope

Zuan Chen[1], Yu Zhou[2], Jingbin Lu[2, *], Shenwen Qi[1], Songfeng Guo[1], Shuaihua Song[1]

[1]Key Laboratory of Shale Gas and Geoengineering, Institute of Geology and Geophysics, Chinese Academy of Sciences, Beijing, China

[2]Central Yunnan Water Diversion Engineering Co., Ltd., Kunming, China

Email address:

zachen@mail.iggcas.ac.cn (Zuan Chen), LJB86784334@qq.com (Jingbin Lu)

[*]Corresponding author

Abstract: Rock fracture and its failure with time due to external forces and other factors such as fluids, temperature have always been a major concern in rock engineering and construction. Based on thermodynamics and theory of solid physics, authors propose an energy criterion for rheological failure of rock, which considers two effects: (1) energy dissipation of rock reduces strength of rock; (2) confining pressure increases strength of rock. Subsequently, we apply it to stability analysis of natural high slope, in order to indicate influence of long time rheology during geology process on material strength and stability of slope. After giving an equation of upper limit estimate for failure time of slide surface in slope, according to viscoelastic solution of stress about high slope under action of gravity, we calculate the relation between sliding time and dip angle (assuming slide line as straight line) and the relation between sliding time and corresponding slid radius (assuming slide line as arc. The minimum time is 10^5 years older. The distribution of contour lines for failure time at each point on the slope shows that points near the slope face have shorter failure times. The results explain topographic feature of high mountains in some extent and indicate that rheological failure of rock also is one of causes for topography forming of slope. It also indicates that the energy criterion for rheological failure of rock provides a base for rheological failure analysis relating to time.

Keywords: Rheological Failure, Energy Criterion, High Slope, Stability, Topographic Feature

1. Introduction

Rock fracture and its failure due to external forces and other factors such as fluids, temperature, and time have always been a major concern in rock engineering and construction. To date, research on rock fracture mechanisms and failure criteria can be conducted from three perspectives: microscale, mesoscale, and macroscale.

At the microscale, some researchers have attempted to deduce the strength of materials based on molecular and crystal structure theories, but the results yielded values significantly higher than those obtained from laboratory experiments. This realization led to the understanding that numerous factors influence the actual strength of materials. For rocks, these factors mainly include pores, porosity, cracks, the curvature radius of crack tips, grains, and grain boundaries.

The study of how these factors affect the strength of rocks forms the basis of the microscale theory of rock strength.

The macroscopic study of rock fracture began earliest. As early as the 17th century, Galileo proposed the maximum principal stress theory. In 1773, Coulomb proposed the Coulomb-Mohr criterion, which was further developed by Mohr in 1900. These theories were experimentally validated and supported within certain ranges. In 1921, Griffith proposed the Griffith theory of brittle fracture in rocks based on the concept of progressive failure and crack-controlled fracture. This theory achieved some success in explaining the mechanisms of crack-opening fracture propagation [10]. Based on experimental data, Hoek and Brown proposed a nonlinear failure criterion for rocks that matched the experimental results well [8]. Subsequently, a large amount of research work enriched and improved these theories of rock strength [7, 18].

Regarding time-dependent rock mechanics issues, in the 1980s, the esteemed Chinese scientist Tjongkie Tan proposed the theory of rock rheology and dilatancy, emphasizing that rocks can undergo dilatancy due to the development of microcracks under differential stress, leading to time-dependent rock failure or earthquakes. This theory has been applied in the analysis of large deformations in Jinchuan tunnels and stability analysis of the Fushun West open-pit mine [5, 2]. In recent years, scientists and engineers have conducted extensive research through field observations, laboratory creep experiments, and computer numerical simulations, proposing various analytical methods [6, 11, 14, 4, 19]. However, there is still no definitive failure criterion for time-dependent rheological failure [3].

This paper presents a universally applicable failure criterion for static, dynamic, elastic-plastic, and rheological conditions from the perspective of energy change, based on the fundamental laws of thermodynamics and solid-state physics. It is applied to the analysis of stability in natural high slopes, aiming to illustrate the influence of rock rheological properties on mountainous landscapes.

2. Energy-Based Failure Criterion for Rock Failure

Currently, the most commonly used criterion for rock fracture in rock mechanics is the Coulomb-Mohr criterion. However, for rheological failure, an energy-based criterion is more convenient.

According to the second law of thermodynamics [12], we have:

External work input = Strain energy + Dissipation energy   (1)

From solid-state physics [9], it is known that when a material fails, we have:

External work input = Cohesive energy + External stress influence function + Surface energy   (2)

Here, the external stress influence refers to the fact that stress (such as confining pressure) increases the strength of the material.

Based on this, the expression of the energy-based failure criterion for rock can be stated as follows:

(1) During the action of external forces on the rock, the dissipation energy inside the rock reduces the cohesive energy of the material by the same amount.

(2) The action of external forces on the rock has two effects: it promotes the development of rock towards failure and enhances the rock's resistance to failure.

(3) When the shear strain energy inside the rock satisfies the following equation, the rock will fail:

$$W = W_0 - \int \sigma_{ij} d\varepsilon_{ij}^p - \int \sigma_{ij} d\varepsilon_{ij}^v + f(\sigma_{ij}) \qquad (3)$$

$W = \dfrac{1}{2G} S_{ij} S_{ij}$ represents the shear strain energy, S_{ij} represents the stress components, G is the shear modulus, W_0 is the sum of material cohesive energy and surface energy, which can be obtained from uniaxial compression-shear failure tests performed prior to failure, representing the elastic energy applied before failure. The second and third terms on the right-hand side represent plastic dissipation energy and rheological dissipation energy, respectively. In the examples where this criterion is applied in this paper, plastic dissipation energy will be neglected. The last term $f(\sigma_{ij})$ is the influence function of stress state on the cohesive strength of the rock. For deep Earth conditions with high confining pressure, the influence of stress on strength must be considered.

3. Stability Analysis of Natural High Slopes

The phenomenon of deformation and subsequent failure of slopes over time is widely observed. By combining field instrument monitoring with numerical calculations, it is possible to predict the evolution and landslide process of slopes over time. However, this requires significant manpower and resources. Providing a theoretical analysis would be beneficial in deepening our understanding of the deformation and failure of slopes over time, making it highly valuable. High slopes are commonly found in high mountain ranges, such as the Qinghai-Tibet Plateau region. Therefore, stability analysis of high slopes is of great importance. Chai Jianfeng et al. [1] analyzed the characteristics of deep cracks in high and steep slopes in mountainous canyon areas. The focus of this paper on high slopes is because they approximately satisfy the geometric and boundary conditions of stress and displacement fields, making it easier to obtain analytical solutions. This section will be divided into the following two parts: 1) Solving the viscoelastic solutions for the stress and displacement fields of high slopes; 2) Calculating the time for slip failure along a predefined slip surface within the high slope to determine the final slip surface and failure time.

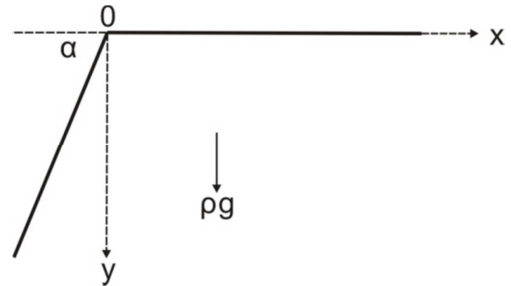### 3.1. Viscoelastic Solutions for High Slopes Under Gravity

Figure 1. *Sketch map of the high slope.*

Consider the high slope shown in Figure 1, where the height is sufficiently large that the geometric shape of its toe has

minimal influence on the stress field in the upper part of the slope. The slope medium is assumed to be homogeneous, isotropic, and possesses certain rheological characteristics. It is subjected to vertical downward gravity. The stress field in the upper part of this slope, according to Saint-Venant's principle, can be approximated as the stress field of an infinitely deep inclined plane.

Assuming the problem is a two-dimensional plane strain problem, the boundary value problem can be described as follows [16]:

Equilibrium equations:

$$\frac{\partial \sigma_x}{\partial x} + \frac{\partial \tau_{xy}}{\partial y} = 0$$
$$\frac{\partial \sigma_y}{\partial y} + \frac{\partial \tau_{xy}}{\partial x} + Y = 0 \tag{4}$$

Here, σ_x, σ_y, and τ_{xy} represent the stress components, and Y represents the body force, i.e., the unit weight.

Geometric equations:

$$\varepsilon_x = \frac{\partial u}{\partial x}, \varepsilon_y = \frac{\partial v}{\partial y}, \gamma_{xy} = \frac{\partial v}{\partial x} + \frac{\partial u}{\partial y} \tag{5}$$

Here ε_x, ε_y, γ_{xy} represent the strain components, and u, v are the displacement components.

Constitutive equations:

Kelvin model: $S_{ij} = Ge_{ij} + \eta \dfrac{de_{ij}}{dt}, \sigma_{ii} = 3K\varepsilon_{ii}$ (6)

Maxwell model: $S_{ij} + \dfrac{\eta}{G} \dfrac{dS_{ij}}{dt} = \eta \dfrac{de_{ij}}{dt}, \sigma_{ii} = 3K\varepsilon_{ii}$ (7)

Here, S_{ij}, e_{ij} are the deviatoric stress and deviatoric strain, $\sigma_{ii}, \varepsilon_{ii}$ are the volumetric stress and volumetric strain, and t represents time.

G, K, η are material constants.

Boundary conditions:

$$\text{At } y = 0, \sigma_y = 0, \tau_{xy} = 0 \tag{8}$$

$$\text{At } y = -x \tan\alpha, \overline{X} = \overline{Y} = 0 \tag{9}$$

Here, α is the slope angle; $\overline{X}$, $\overline{Y}$ represents the stresses in the x and y directions on the slope surface.

Based on the correspondence principle, the above viscoelastic boundary value problem can be solved using the corresponding elastic solution through Laplace transformation.

From the theory of elasticity, for the corresponding elastic problem, we take the stress function as

$$\phi = ax^3 + bx^2y + cxy^2 + dy^3 \tag{10}$$

It clearly satisfies the biharmonic equation

$$\nabla \cdot \nabla \phi = 0 \tag{11}$$

Therefore,

$$\sigma_x = \frac{\partial^2 \phi}{\partial y^2} = 2cx + 6dy$$
$$\sigma_y = \frac{\partial^2 \phi}{\partial x^2} - Yy = 6ax + 2by - \rho gy \tag{12}$$
$$\tau_{xy} = -\frac{\partial^2 \phi}{\partial x \partial y} = -2bx - 2cy$$

By applying the boundary conditions, the final stress solution is given by

$$\sigma_x = -\rho g \cot\alpha x$$
$$\sigma_y = -\rho gy \tag{13}$$
$$\tau_{xy} = \rho g \cot\alpha y$$

Since the above equation is independent of material properties, it is also a stress field solution for viscoelastic media.

3.2. Estimation of Failure Time and Determination of Sliding Surface for Natural High Slopes

Once we have the stress and strain fields, it is natural to use them to predict the stability of the slope. However, the actual situation is highly complex. Before a slope can potentially fail, it generally undergoes processes such as crack initiation, crack propagation, and eventually sliding. These processes cannot be captured by our analytical solutions.

Here, we aim to overcome these difficulties by utilizing the energy failure criterion proposed in the previous section and the analytical solution presented in section 3.1. Under certain assumptions, we seek to obtain an upper limit estimate for the potential failure time of the slope.

Assumptions:

(1) The potential sliding surface of the slope is a smooth curve, which can be considered a smooth line in the two-dimensional case.

(2) When the total shear strain energy and dissipated energy on the sliding surface are equal to the total potential energy and surface energy on the sliding surface, the sliding surface experiences overall failure and sliding occurs.

(3) The sliding surface that has the minimum failure time among all potential sliding surfaces is considered to be the first failure surface.

In the depicted slope shown in Figure 2, let's assume a potential sliding line (in two dimensions) denoted as L. The total potential energy and surface energy on L are obtained by integrating the potential energy and surface energy $W_0(x,y)$ at each point on the line, given by

$$\overline{W_0} = \int_L W_0(x, y) dl \tag{14}$$

The elastic shear energy on L is given by

$$\overline{W} = \int_L \frac{1}{2G} S_{ij} S_{ij} dl \tag{15}$$

The time-dependent dissipative energy, disregarding instantaneous plastic dissipation, is given by

$$\overline{W_c} = \int_L \int_0^t \sigma_{ij} \frac{d\varepsilon_{ij}}{dt} dt \tag{16}$$

The influence of stress on cohesive strength is described as

$$\overline{f(\sigma_{ij})} = \int_L f(\sigma_{ij}) dl \tag{17}$$

The fracture criterion is expressed as

$$\overline{W} = \overline{W_0} - \overline{W_c} + \overline{f(\sigma_{ij})} \tag{18}$$

When the above condition is satisfied, the sliding surface will experience sliding.
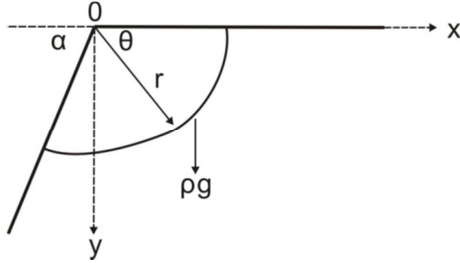

Figure 2. *Sketch map of assumed slid surface.*

There are various possible shapes for the potential sliding line, such as straight lines and circular arcs.
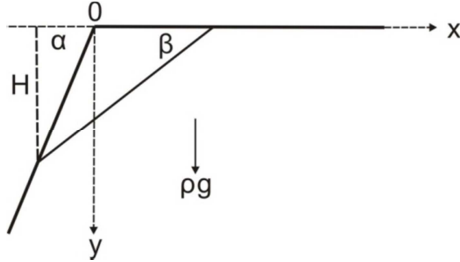

Figure 3. *Sketch map of straight line slide line.*

As shown in Figure 3, with the slope angle $\alpha = 45°$, let's assume the sliding line to be a family of straight lines, given by the equation:

$$y = -\tan \beta x + k \tag{19}$$

Taking $\rho g = 2.7$ g/cm³ and $\mu = 0.25$, the stress solution is given by:

$$\sigma_x = -2.7x, \sigma_y = -2.7y, \sigma_z = 0.25(\sigma_x + \sigma_y), \tau_{xy} = 2.7y \tag{20}$$

Note that the stress is independent of time. For the Maxwell model, the strain is given by [17]:

$$e_{ij} = S_{ij}\left(\frac{1}{G} + \frac{t}{\eta}\right) \tag{21}$$

$$\varepsilon_0 = K\sigma_0$$

Thus,

$$W(x, y) = \frac{1}{2G} S_{ij} S_{ij} = \frac{1}{2G}\left(ax^2 + bxy + cy^2\right)$$
$$a = 3.94875, b = -6.1875, c = 11.42775 \tag{22}$$

$$W_c(x, y) = \int_0^T S_{ij} \frac{de_{ij}}{dt} dt = S_{ij} S_{ij}\left(\frac{1}{G} + \frac{t}{\eta}\right)\Big|_0^T$$
$$= \frac{2G}{\eta} W(x, y)T \tag{23}$$

Integrating along the straight segment in the slope, we obtain:

$$\overline{W} = \int_L W(x, y) dl$$
$$= \int_0^H \frac{1}{2G}\left(ax^2 + bxy + cy^2\right)\Big|_{y = -\tan \beta x + k}\left(\sqrt{1 + \cot^2 \beta}\right) dy \tag{24}$$
$$= \frac{1}{2G\sin \beta}(D_1 H + D_2 H^2 + D_3 H^3)$$

where

$$D_1 = \frac{ak^2}{\tan^2 \beta}$$

$$D_2 = -\frac{ak}{\tan^2 \beta} + \frac{bk}{2\tan \beta} \tag{25}$$

$$D_3 = \frac{a}{3\tan^2 \beta} - \frac{b}{3\tan \beta} + \frac{c}{3}$$

$$\overline{W_c} = \int_L W_c(x, y) dl$$
$$= \int_L \frac{2GT}{\eta} W(x, y) dl \tag{26}$$
$$= \frac{2GT}{\eta} \overline{W}$$

Assuming the slope to be a homogeneous medium with a constant cohesion energy W0, we have:

$$\overline{W_0} = \int_L W_0 dl = \frac{W_0 H}{\sin \beta} \tag{27}$$

If we take

$$f(\sigma_{ij}) = -\lambda(\sigma_x + \sigma_y + \sigma_z)^3 \tag{28}$$

then

$$f(\sigma_{ij}) = 38.44\lambda(x + y)^3$$

$$\int_L f(\sigma_{ij})dl = 38.44\lambda(A_1H + A_2H^2 + A_3H^3 + A_4H^4)$$

$$A_1 = \frac{k^3}{\tan^3\beta}, A_2 = \frac{3k^2}{2\tan^3\beta}(1-\tan\beta),$$

$$A_3 = \frac{k}{\tan^3\beta}(1-2\tan\beta+\tan^2\beta),$$

$$A_4 = \frac{1}{4\tan^3\beta}(-1+3\tan\beta-3\tan^2\beta+\tan^3\beta)$$

(29)

Substituting equations (24), (26), (27), and (28) into equation (18), we have:

$$T = \frac{\eta}{2G}\left(\frac{\overline{W_0}+\overline{f(\sigma_{ij})}}{\overline{W}}-1\right)$$

(30)

From the above equation, we can see that as H increases, T also increases, which is consistent with logic. This is also the reason for choosing the form of (28) of. $f(\sigma_{ij})$

Assuming the rock type of the slope to be basalt, the uniaxial compressive strength is approximately $\sigma_f = 300$ MPa, and the elastic modulus E = 4.0 x 10^4 MPa [13]. Thus, $w_0 = \frac{\sigma_f^2}{2E} = 1.125MPa$. In this paper, we take $\lambda = 10^{-5} MPa^{-2}$ and $\eta = 10^{20} Pa \cdot s$.
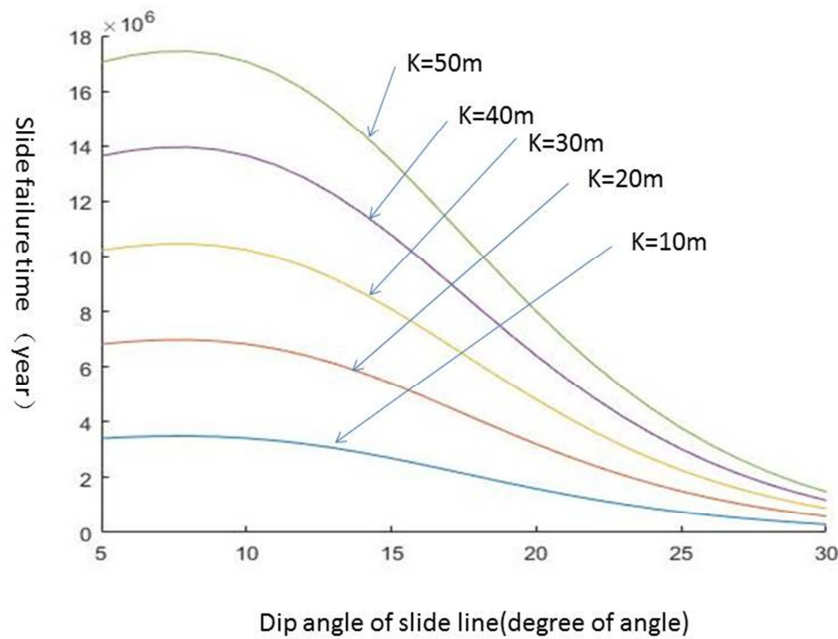

Figure 4. Relation between slide failure time and dip angle of slide line when slide line is assumed as straight line.

Under the given parameters, when the sliding line is straight, the relationship between the sliding failure time and the inclination angle of the sliding line is shown in Figure 4 for different values of k (the intercept of the sliding line on the Y-axis). It can be observed from the graph that as k increases, the failure time becomes longer. Additionally, as the inclination angle of the sliding line increases, the failure time decreases. Calculations show that for k = 10m and H = 23.6m,

the shortest failure time is 2.9×10^5 years.

If we assume that the sliding line is an arc with the slope vertex as the center and a radius of r, i.e.,

$$x = r\cos\theta, y = r\sin\theta, 0 \le \theta \le 180^0 - \alpha \qquad (31)$$

then

$$\overline{W} = \int_0^{180^0-\alpha} \frac{r^2}{2G}\left(a\cos^2\theta + b\cos\theta\sin\theta + c\sin^2\theta\right)rd\theta$$

$$= \frac{r^3}{4G}\left[(a+c)\sin(2\alpha)+b\sin^2\alpha+c(180^0-\alpha)\right]$$

(32)

$$\overline{f(\sigma_{ij})} = 38.44\lambda\int_0^{180^0-\alpha} r^3\left(\cos^3\theta - 3\cos^2\theta\sin\theta + \cos\theta\sin^2\theta - \sin^3\theta\right)rd\theta$$

$$= 38.44\lambda r^4\left(\frac{2}{3}\cos^3\alpha + \sin\alpha + \cos\alpha + \frac{5}{3}\right)$$

(33)

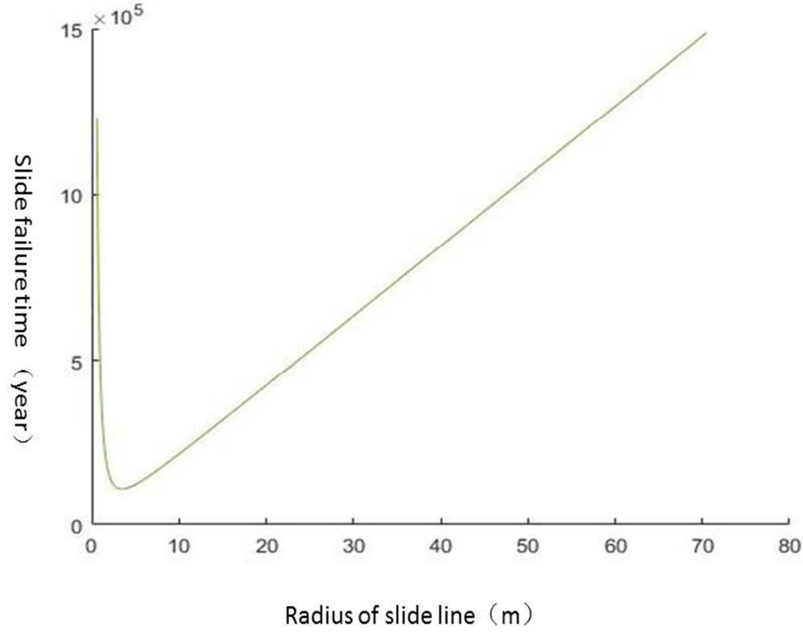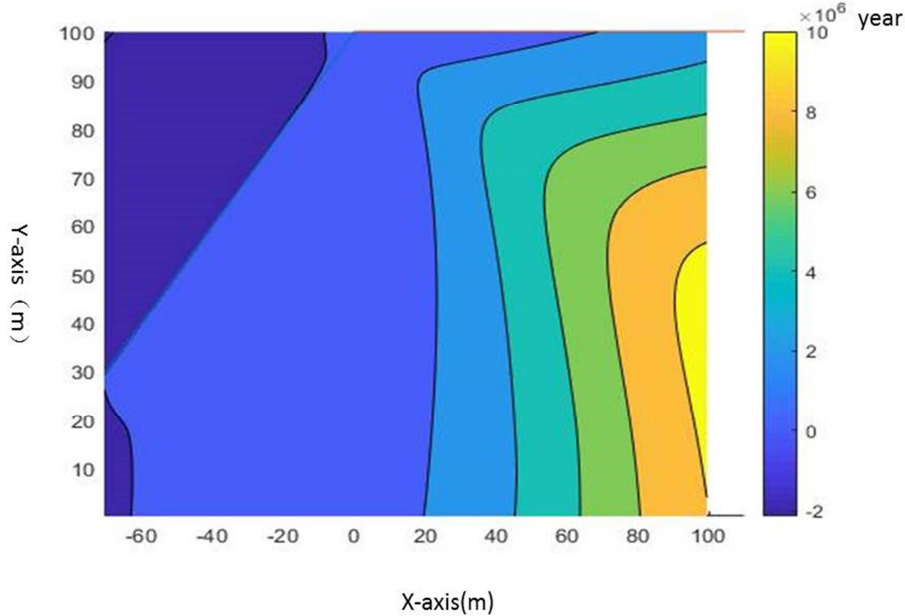$$\overline{W_0} = w_0(\pi-\alpha)r \qquad (34)$$

Figure 5. *Relation between slide failure time and radius of slide line when slide line is assumed as arc.*

Under the same parameters, according to formula (30), the calculation for the sliding failure time when the sliding line is an arc is shown in Figure 5. It can be observed from the graph that as the radius of the sliding line increases from zero, the failure time initially decreases and then increases. The shortest failure time is 10^5 years, which occurs when the radius of the sliding line is 3.5 meters.

Under the same parameters, the failure time at each point on the slope is calculated using the following equation:

$$T = \frac{\eta}{2G}\left(\frac{W_0 + f(\sigma_{ij})}{W} - 1\right) \qquad (35)$$

The distribution of contour lines is shown in Figure 6. From the graph, it can be observed that points near the slope face have shorter failure times. Therefore, the rock properties near the edge of the slope are more prone to weakening, making them susceptible to landslide under external forces.

(Zero point of ordinate is located at 100m depth below the surface, the abscissa is the same as in figure 1)

Figure 6. *Contour line distribution map of failure time of points in slope.*

In reality, it is also possible that a specific point initially meets the failure criterion, leading to local failure and the formation of cracks. Subsequently, these cracks may propagate over time, eventually resulting in a landslide.

4. Discussion

4.1. Determination of Parameters in the Failure Criterion

The rheological failure criterion proposed in this study requires knowledge of parameters such as elastic modulus, Poisson's ratio, viscosity constant, uniaxial failure strength, and the coefficient of static hydrostatic pressure influence. These parameters can be determined through uniaxial tests, creep tests, and triaxial tests. Uniaxial tests can determine the rock's elastic modulus, Poisson's ratio, and compressive strength. Creep tests can determine the rock's viscosity. Triaxial tests under different confining pressures can determine the coefficient of static hydrostatic pressure influence. It is also possible to infer the rheological properties of rocks through geophysical observations, such as viscosity parameters. Due to the gradual process of energy rheological dissipation, especially in shallow layers with lower temperatures, the calculated failure times are generally long.

4.2. Geological Significance of Determining Natural High Slope Failure Time

Natural high slopes are formed naturally during geological processes and have a long history. For example, mountains in the Qinghai-Tibet Plateau region have existed for tens of millions of years [15]. Due to various factors, including tectonic uplift, erosion also plays a role in maintaining dynamic equilibrium during the uplift of mountainous areas. Based on the calculations in this study, we found that after the formation of a high mountain, it takes approximately 100,000 years for a circular rupture slip plane to form at a depth of approximately 3.5 meters below the surface due to rock rheology. Subsequently, under the influence of gravity, sliding may occur, resulting in a landslide. For a linear slip line, the shortest failure time occurs at a depth of 23 meters where the line intersects with the slope surface, but it still requires 300,000 years. This explains why the tops of high mountains are generally pyramid-shaped. The calculations also indicate that points near the slope surface have shorter failure times, suggesting that they are more susceptible to weakening and the formation of cracks under external forces. The calculations indirectly suggest that a circular slip line dissipates energy faster than a linear slip line.

Although the medium in the interior of the slope undergoes energy dissipation and experiences changes in microstructure under the influence of gravity, it does not necessarily lead to a landslide but rather indicates a deterioration in rock quality. Additionally, the calculated failure times for slip lines or individual points are on the order of hundreds of thousands of years, which is relatively short compared to geological history. In this context, "failure" does not mean complete fragmentation of the rock, but rather the generation of microcracks at a certain scale. Further calculations would require adjusting the rock material parameters to enter a new cycle.

4.3. Practical Significance of the Rheological Energy Failure Criterion

Once the initial state of the target of the study is determined, the rheological energy failure criterion can be applied to determine the failure time at the examined points. In addition to using analytical solutions as demonstrated in this study, numerical solutions are also feasible. Computers provide the possibility for long-term calculations. The rheological energy failure criterion establishes a foundation for time-dependent rheological analysis.

5. Conclusion

Based on the fundamental laws of thermodynamics and solid physics, this study proposed an energy rupture criterion for rock rheology and applied it to the stability analysis of natural slope landslides. By using the viscoelastic solutions for high slopes under the influence of gravity, we calculate the relation between sliding time and dip angle (assuming the slide line is a straight line) and the relation between sliding time and corresponding slid radius (assuming the slide line as arc. The minimum time is 10^5 years older. The distribution of contour lines for failure time at each point on the slope shows that points near the slope face have shorter failure times. Therefore, the rock properties near the edge of the slope are more prone to weakening, making them susceptible to landslide under external forces. This partially explains the formation of the geomorphic characteristics of high mountains. Moreover, the results indicate that the rheological energy failure criterion lays the foundation for time-dependent rheological analysis.

Acknowledgements

References

[1] Chai, J. F., Qi, S. W., Ten, K. S., Long, X., 2007. Special Characteristics of Deep Fractures in High and Steep Slopes in Southwestern of China. Journal of Engineering Geology, 17 (4), 730-738.

[2] Chen, Z., 1994. Rheological Analysis of Stability on North Side Slope of Western Open Mine at Fushun. Thesis Collection of Third Session Conference for Rock Mechanics and Engineering.

[3] Chen, Z., Li, M., 2019. Is there any rheological failure for material inside earth interior due to long time action at low stress? Progress in Geophysics (in Chinese), 34 (1), 1-5.

[4] Chen, Z., Jin, Z., Huang, X., Qi, S., 2022. A Damage Mechanics Analysis on Rheological Failure of Rocks under High Temperatures and Pressures. American Journal of Physics and Application, 10 (2), 24-32.

[5] Tan, Z., Kang, W., 1983. Time Dependent Dilatancy Prior to Rock Failure and Earthquake. Chinese Journal of Rock Mechanics and Engineering, 2 (1), 11-21.

[6]   Cui, X. H., Fu, Z. L., 2006. Experimental Study on Rheology Properties and Long Term Strength of Rocks. Chinese Journal of Rock Mechanics and Engineering, 25 (5), 1021-1024.

[7]   Guo, S.. Qi, S., Zhan, Z., Zheng, B., 2017. Plastic- strain-dependent strength model to simulate the cracking process of brittle rocks with an existing non-persistent joint, Engineering Geology, 231, 114-125.

[8]   Hoek, E., Carranza-Torres, C., Corkum, B., 2002. Hoek-Brown failure criterion-2002 edition. In: Proceedings of NARMS-Tac, 1, pp. 267-273.

[9]   Huang, K, Han R. Q., 2019. Solid state physics. Science Press.

[10] Jaeger, J. C., Cook, N. G. W., 1981. Fundamentals of Rock Mechanics. Science Press.

[11] Wang, X. D., Fu, X. M., 2009. Numerical Simulation Test for Physical Compress Creep Experiment. Journal of Engineering Geology, 17 (4), 533-537.

[12] Wang, Z. X., 1960. Thermodynamics. Higher Education Press.

[13] Tang, D. X., Liu Y. R., Zhang, W. S., Wang Q., 1998. Engineering Geotechnics. (Second Edition) Geological Publishing House.

[14] Xu, Q., 2012. Theoretical Studies on Prediction of Landslides Using Slope Deformation Process Data. Journal of Engineering Geology, 20 (2), 145-151.

[15] Xu, Q., Ding, L., 2015. Paleoelevation research on Gangdise Mountains and Qinghai Tibet Plateau. China Science Foundation.

[16] Xu, Z. L., 1979. Elastic mechanics. People's Education Press.

[17] Yin, X. C. 1988. Solid Mechanics. Seismological Publishing House.

[18] Zhu, Q. Z., 2017. A new rock strength criterion from microcracking mechanisms which provides theoretical evidence of hybrid failure. Rock Mechanics and Rock Engineering, 50 (2): 341-352.

[19] Zhu, Q., Li, T., Zhang, H., Ran, J. et al., 2022. True 3D Geomechanical Model Test for Research on Rheological Deformation and Failure Characteristics of Deep Soft Rock Roadways. Tunnelling and Underground Space Technology, Vol. 128, October 2022, 104653.